JOURNAL OF SYNCHROTRON RADIATION

ISSN 1600-5775

Received 15 July 2020
Accepted 12 October 2020

Edited by S. M. Heald, Argonne National Laboratory, USA

Keywords: photoelectron shield; soft X-ray beamline; first-mirror chamber; heat load.

Photoelectron shield for the first mirror of a soft X-ray beamline

Daisuke Wakabayashi,[a,b]* Hirokazu Tanaka,[a] Akio Toyoshima,[a] Shohei Yamashita[a,b] and Yasuo Takeichi[a,b]

[a]Institute of Materials Structure Science, High Energy Accelerator Research Organization (KEK), Tsukuba, Ibaraki 305-0801, Japan, and [b]Department of Materials Structure Science, Graduate University for Advanced Studies, Tsukuba, Ibaraki 305-0801, Japan. *Correspondence e-mail: daisuke.wakabayashi@kek.jp

At a soft X-ray beamline with an undulator source, significant heat generation at the first-mirror chamber and light emission at the viewport were found, which can be explained by photoelectrons from the mirror. The chamber temperature increases up to approximately 50°C over a period of several hours. A photoelectron shield consisting of thin copper plates not only prevents the heat generation and light emission but also improves the pressure of the vacuum chamber, if a voltage of a few tens of V is applied to the shield. The total electron yield of the shield reached as much as 58 mA under high heat-load conditions, indicating the emission of numerous photoelectrons from the first mirror. Heat-balance analyses suggest that approximately 30% or more of the heat load on the first mirror is transferred to the surroundings.

1. Introduction

The heat load on X-ray optics such as mirrors, gratings and crystals has a strong effect on the performance of synchrotron beamlines. As significant progress in synchrotron radiation sources has increased brilliance, techniques to solve the problems of heat load have been developed over a long period (*e.g.* Freund *et al.*, 1990; Becker, 1992; Bilderback *et al.*, 2000). In particular, it is difficult to reduce the heat load at soft X-ray beamlines, because the high-pass filters made of beryllium or graphite that are often installed at hard X-ray beamlines cannot be used. Instead, the first mirror of the beamline practically acts as a low-pass filter on selection of a suitable coating material and incidence angle (*i.e.* adjusting the critical energy). The radiated power of a typical undulator reaches an order of kW at third-generation soft X-ray synchrotron radiation sources (Schlachter & Wuilleumier, 1994). A flat first mirror has been installed at some beamlines for the purpose of removing the heat load (*e.g.* Ohresser *et al.*, 2014; Belkhou *et al.*, 2015). Therefore, it is important to impose an appropriate heat load on the first mirror and cool it effectively.

At the Photon Factory, a new soft X-ray beamline with an undulator source, BL-19A/B, has been constructed. The commissioning of BL-19A/B showed that there was significant heat generation at the first-mirror chamber. Over a period of several hours, the chamber temperature changed with changes in the undulator's parameters (*i.e.* gap and polarization mode) and in the size of the slits located upstream. The walls on the side of the mirror surface were particularly affected and the temperature reached as high as 50°C. In addition, significant light emission was found at the viewport on the side of the mirror surface, together with the heat generation. Fig. 1 shows the light emission at the viewport when irradiating the mirror.

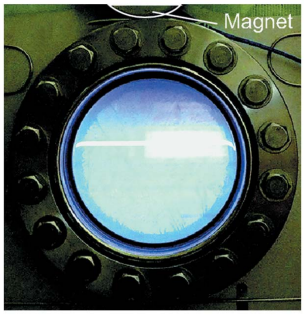

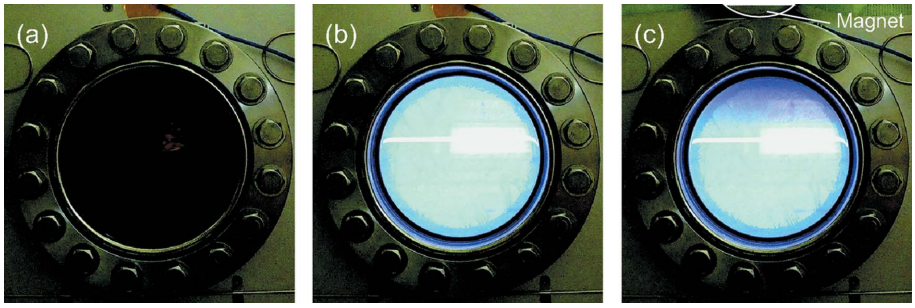

Figure 1
Light emission at the viewport of the first-mirror chamber of BL-19A/B: (*a*) without X-rays, and (*b*) and (*c*) with X-rays. In (*c*), a magnet is placed above the viewport flange. Charged particles such as electrons are trapped by the magnetic field and therefore removed in the vicinity of the magnet. Also, an X-ray path and part of the mirror seem to emit light (see discussion in Section 4.1).

The light-emission distribution could be modified by a magnet placed in the vicinity, as shown in Fig. 1(*c*), indicating that the light emission is caused by charged particles such as electrons. These observations suggest that photoelectrons emitted from the first mirror cause both the heat generation and the light emission.

The heat load on the first-mirror chamber degrades the beamline performance. Over a period of several hours, it indirectly changes the temperatures of the mirror stages and holder, causing beam drift and a resultant energy shift at the experimental station. Heat generation at the first-mirror chamber has been commonly observed with other soft X-ray beamlines of the Photon Factory. Although many researchers have sought techniques to address the problems of the heat load on mirrors, there have been few reports on the heat load transferred to the surroundings by photoelectrons. It has been reported that a cooled shield (called a Compton shield) is installed for a first mirror at a hard X-ray beamline of the European Synchrotron Radiation Facility (Mairs *et al.*, 2010). At soft X-ray beamlines of a 3 GeV class source, such as the Photon Factory, the heat load by photoelectrons may be dominant over that by scattered X-rays. In addition, carbon contamination of optics is often a problem with soft X-ray beamlines (*e.g.* Boller *et al.*, 1983), and it has been pointed out that photoelectrons or X-rays emitted from a mirror may be the cause (Ohashi *et al.*, 2016). To gain a better understanding, it is necessary to clarify the existence of photoelectrons and estimate them quantitatively. In this study, we designed and installed a photoelectron shield for the first-mirror chamber and evaluated its performance. We also measured the total electron yield of the shield, and discussed the heat balance of the first mirror.

2. Design

The design of the photoelectron shield is shown in Fig. 2. It consists of copper plates with a thickness of 1 mm (except for the ceiling plate, which is 3 mm thick, to ensure strength). To achieve high vacuum conditions, the shield was baked at 150°C before installation. It was hung from the top board of the chamber and set at a distance of 20–30 mm from the inner wall with dimensions of 260 mm (V) × 440 mm (H) × 370 mm (D), to receive photoelectrons and X-rays emitted from the inside mirror with dimensions of 250 mm (L) × 30 mm (W) × 30 mm (T). Copper tubes were bonded to the ceiling of the shield and used for a cooling water circuit via a port on the top board. Insulators were positioned at the bolts connecting the shield to the top board and at the flange for the cooling pipes, in order to insulate the shield from the chamber, enabling us to measure the total electron yield of the shield. Downward-emitted photoelectrons are likely to heat the mirror holder and stages directly, and therefore a copper plate with a thickness of 1 mm was set just under the cooling block, which removes the heat load on the plate as well as that on the

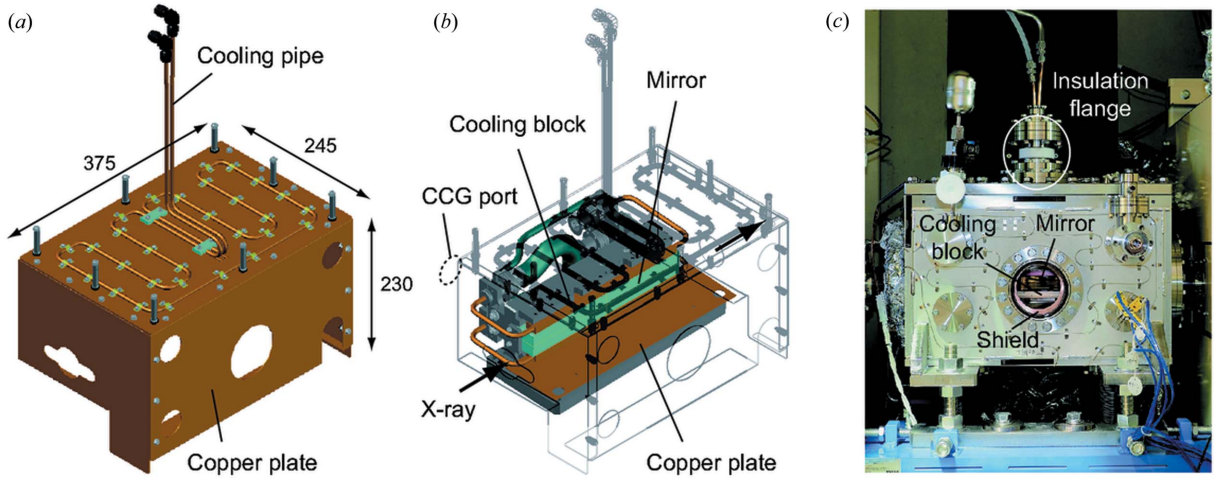

Figure 2
Design of the photoelectron shield and photograph of the mirror chamber. The schematic illustrations show (*a*) the shield only, and (*b*) the mirror and holder inside the shield. The numbers represent the dimension in units of mm. (*c*) A photograph taken in the direction of the viewport. The copper plate of the shield, the mirror surface and the cooling blocks can be partly seen through the viewport. A flange with its white-coloured insulator is set at the top of the chamber, to introduce the cooling pipes.

mirror [Fig. 2(*b*)]. In addition, the shield has windows for the ports of the chamber, which enable us to observe the mirror surface through a viewport. A photograph of the mirror chamber after installing the shield is shown in Fig. 2(*c*). The mirror surface and part of the shield can be seen through the viewport. It is important to confirm the condition of the mirror surface (*e.g.* carbon contamination) visually, for maintenance purposes.

3. Performance evaluation

The photoelectron shield was installed in the first-mirror chamber of BL-19A/B at the Photon Factory with an electron storage ring energy of 2.5 GeV and a current of 450 mA. The details of BL-19A/B will be published in a dedicated paper currently in preparation. An APPLE-II-type undulator (Sasaki *et al.*, 1993) is used as the source point of BL-19A/B. The performance evaluation was conducted under a highest heat-load condition (*i.e.* a linear horizontal polarization mode at K = 4.5). The current measurements explained below were conducted under the highest heat-load condition and a lower heat-load condition (*i.e.* a linear horizontal polarization mode at K = 1.5). A photon beam was shaped to 2.5 mm (V) and 5.0 mm (H) with a quadrant slit at a distance of 11.9 m from the source. It irradiated the first mirror at a distance of 12.6 m from the source. The power of incident X-rays is estimated to be 560 and 160 W under the high and lower heat-load conditions, respectively. The mirror was made of pure silicon coated with gold and its grazing angle was 1.6°. A chiller was connected to the cooling blocks of the mirror and maintained the temperature and flow rate of cooling water at 25°C and 0.5 l min^{-1}, respectively. The shield was cooled with water supplied throughout the facility, the temperature and flow rate of which were monitored with gauges connected to the cooling pipes.

Temperature measurements of the chamber were conducted with type-K thermocouples mounted on the chamber wall facing the mirror surface (front) and on the opposite chamber wall to the rear of the mirror. The time evolution was recorded from shutter opening after settling the temperature of the first-mirror system sufficiently without a beam. An electrode was placed at the flange for cooling pipes connected to the shield, which is insulated from the chamber. By applying voltages from −200 to 200 V, the dependence of the current flowing through the shield was measured. The chamber pressure was measured as a function of the voltage with a cold cathode vacuum gauge (CCG) set at the port on the rear chamber wall [Fig. 2(*b*)].

4. Results and discussion

4.1. First-mirror chamber

The time evolution of the chamber temperature is shown in Fig. 3. The solid and dotted lines represent the temperatures of the front and rear chamber walls corresponding to the side of the mirror surface and to the opposite side, respectively. The

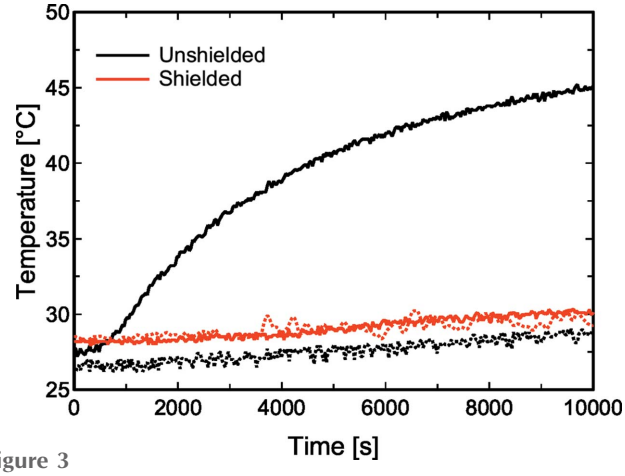

Figure 3
Time evolution of the temperature of the mirror chamber. The solid and dotted lines represent the temperatures on the side of the mirror surface and on the opposite side, respectively. A small discrepancy of ∼2°C can be seen at 0 s, before and after installing the shield. It is due to the change in the room temperature without a beam at the main hutch containing the first-mirror chamber, which may be affected by air-conditioner settings, seasonal changes, positions of heat sources such as pumps *etc.*

data before installing the shield shown as black lines indicate that the side of the mirror surface is locally heated up to approximately 45°C over a period of several hours. In contrast, after installing the shield, only a small temperature rise is observed. No apparent discrepancy is observed between the positions of the chamber, suggesting that the shield could reduce the heat load on the chamber drastically. Photographs of the viewport before and after installing the shield are shown in Fig. 4. The shield suppresses strong light emission at the viewport. The bright horizontal band observed both before and after installing the shield corresponds to the path of the X-ray beam, which is made visible due to emission by a small pressure of oxygen in the chamber for *in situ* removal of carbon contamination on the mirror (*e.g.* Toyoshima *et al.*, 2012; Watts *et al.*, 2018). Strong light is also observed around the mirror surface before installing the shield, which may be due to the reflection of visible light from the viewport. It was shown that the shield can effectively prevent heat generation and light emission of the first-mirror system.

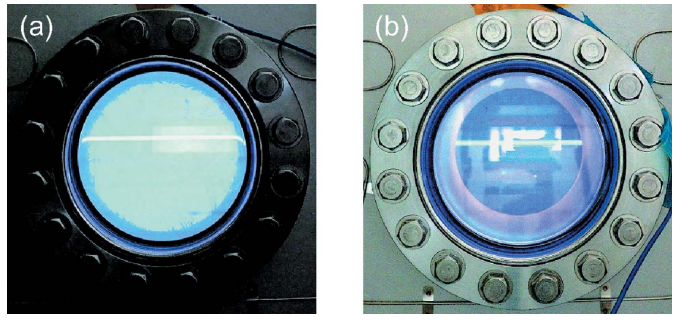

Figure 4
Change in light emission at the viewport of the chamber with the shield. (*a*) and (*b*) are photographs taken before and after installing the shield, respectively. They were corrected for exposure conditions, although the lighting differs. See the text on the origin of each light.

4.2. Photoelectrons

The applied voltage dependence of the current flowing through the shield is shown in Fig. 5. The red and blue symbols represent the results under high and low heat-load conditions, respectively (see Section 3). The current increases with the heat load and reaches as much as 58 mA. Under the high heat-load condition, current measurements could not be conducted above 70 V due to the sourcemeter limitation although one would expect to measure a higher current by applying a higher voltage. The current rapidly increases at around 0 V and almost converges at a few tens of V. In particular, a jump of as much as ∼10 mA in current occurs at around 0 V under the high heat-load condition, and therefore stable current measurements could not be conducted due to the sourcemeter limitation. These observations clarify the existence of numerous electrons (corresponding to 58 mA in current). The pressure data of the chamber are plotted as crosses in Fig. 5. The pressure significantly decreases with an increase in current. The electrons in the chamber may stimulate gas desorption. However, the decrease in pressure may be due to a reduction of the incident electrons to the cold cathode vacuum gauge. In any case, the pressure value of the chamber can be improved by modifying the voltage applied to the shield.

There are two possibilities that would explain the origin of the electrons measured at the shield. One is that photoelectrons emitted from the mirror are captured directly or indirectly. The other is that scattered X-rays yield photoelectrons at the shield. First, the energy of incident X-rays is generally below 10 keV, as discussed later, and therefore the yield of photoelectrons is supposed to be dominant at the Au-coated mirror, compared with that of fluorescence X-rays (Krause, 1979). In addition, while photoelectrons add electrons to the shield and are measured as a positive current, X-rays remove electrons from the shield and are measured as a negative current. Therefore, the sign of the current in Fig. 5 indicates that far more electrons are arriving at the shield than are leaving it. In particular, the current was close to 0 mA at around −200 V. These observations suggest that the origin of the measured current is photoelectrons and not photons from the mirror. It has been pointed out that photoelectrons or X-rays emitted from a mirror stimulate carbon desorption from chamber walls and cause carbon contamination of the mirror surface (Ohashi *et al.*, 2016). Our observations suggest that the main cause is photoelectrons, not X-rays, and that a photoelectron shield can be useful for preventing carbon contamination.

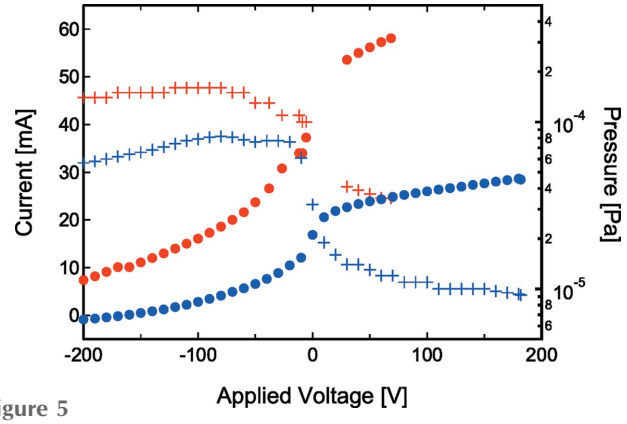

Figure 5
Applied voltage dependence of the current flowing through the shield and the pressure of the mirror chamber. The red and blue symbols represent the results under the high and low heat-load conditions with undulator parameters of K = 4.5 and 1.5, respectively. The circles and crosses represent the current and pressure data, respectively. See the text for the reason for the lack of data under the high heat-load condition.

It seems that Fig. 5 shows the situation where the energy of incident photoelectrons was mainly below 200 eV. However, the current includes the secondary electrons emitted from the shield as well as the incident photoelectrons, meaning that the applied voltage dependence does not directly reflect the energy distribution of the incident photoelectrons. Under the high heat-load condition, the current is below 10 mA at around −200 V, and it rapidly increases at around 0 V and then almost converges to ∼60 mA. It is highly possible that most of the photoelectrons with higher energies (corresponding to ∼60 mA in current) yield secondary electrons with energies of a few to tens of eV at the shield and that the secondary electrons were observed to be repelled (or attracted) by applying a negative (or positive) voltage. By applying a positive voltage of a few tens of V to the shield, they can be prevented from hitting elsewhere in the chamber and causing outgas, which may improve the pressure of the chamber.

4.3. Heat balance

The heat balance of the first mirror under the high heat-load condition is discussed. The power of incident X-rays Q_I is estimated to be 560 W from the parameters of the undulator and the opening of the slits. The power of reflected X-rays Q_R is estimated to be 30 W from the flux of incident X-rays and the reflectance of the mirror. The power and flux of incident X-rays were calculated using *SPECTRA* (Tanaka & Kitamura, 2001) and the reflectance was calculated from previous data (Henke *et al.*, 1993). On the other hand, the powers absorbed at the mirror and at the shield, Q_M and Q_S, are estimated to be 360 and 150 W, respectively, from the change in temperature and the flow rate of the cooling water. The power absorbed at the first-mirror system (*i.e.* not reflected, $Q_I - Q_R$) is 530 W, almost corresponding to the total power absorbed at the mirror and shield of 510 W ($Q_M + Q_S$). The discrepancy of 20 W may suggest that the shield could not remove the heat load completely, but it may be within the error in Q_S, which is estimated to be approximately 10% due to accuracy in the temperature control of the shield-cooling water. These heat-balance analyses suggest that photoelectrons transfer heat corresponding to approximately 30% of the total absorbed heat from the first mirror to the shield, $Q_S/(Q_M + Q_S)$. Here, the heat transferred via the downward-emitted photoelectrons is removed through the cooling blocks of the mirror and is included in Q_M [see Section 2 and Fig. 2(*b*)]. Therefore, it is supposed that the actual proportion of heat transferred by photoelectrons is more than 30%.

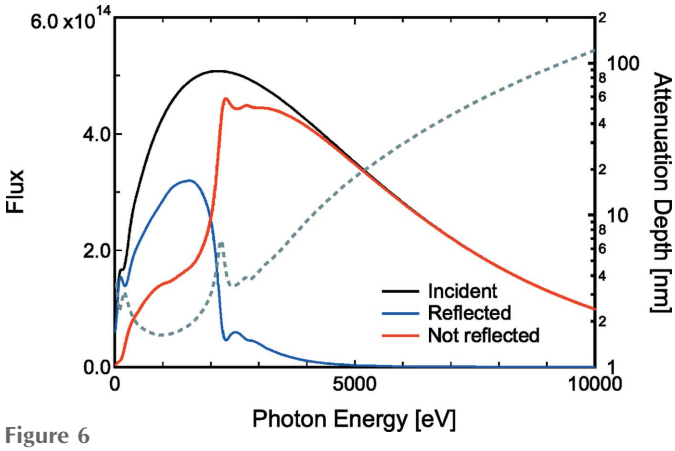

Figure 6
Flux spectrum calculations for X-rays not reflected at the first mirror. The flux of incident X-rays is equal to the sum of the fluxes of X-rays that are reflected and not reflected. The smoothing was made to smear out the interference of undulator radiation. The attenuation depth is also plotted as a grey dotted line for reference.

The medium of the heat transfer from the first mirror to the shield is discussed again. If photoelectrons, corresponding to 58 mA in current, transfer the power of 150 W (Q_S), their energy should be a few keV. The flux spectrum of X-rays which are not reflected at the first mirror is shown in Fig. 6. It is obtained from the difference in fluxes of incident and reflected X-rays. The spectrum shows a maximum at ∼3 keV and the X-rays excite photoelectrons. The attenuation depth from the mirror surface at an incidence angle of 1.6° is calculated from the previous data (Henke *et al.*, 1993) and also shown for reference. It stays within several nanometres from the surface below ∼4 keV and rapidly rises above ∼5 keV. Considering the universal curve of the inelastic mean free path of electrons (*e.g.* Seah & Dench, 1979), photoelectrons with energies in the order of keV at the depth of several nanometres fairly escape the mirror and contribute to the heat transfer. As discussed in Section 4.2, Fig. 5 does not show the energy distribution of the incident photoelectrons from the mirror, which does not contradict our interpretation. In fact, the Q_S estimates (*i.e.* the heat load on the shield) were not changed significantly in our current measurements.

5. Summary

At a soft X-ray beamline with an undulator source, we found heat generation at the first-mirror chamber and light emission at the viewport. It was shown that these phenomena can be explained by photoelectrons emitted from the mirror, and are easily prevented by a shield consisting of thin copper plates. It is supposed that more than 30% of the total heat load on the first mirror is transferred to the surroundings. By applying a positive voltage of a few tens of V to the shield, the secondary electrons can be prevented from escaping from the shield and the pressure of the chamber can be improved. It is expected that they may be attracted more effectively with appropriate arrangements of magnets and/or electrodes. The main cause of photoelectrons is X-rays at energies in the order of keV by high-order harmonics of the undulator radiation (see Fig. 6), suggesting that photoelectron generation at the first mirror is a common issue, particularly for soft X-ray beamlines of a 3 GeV class source. The photoelectron shield should be standard equipment in a first-mirror chamber of soft X-ray beamlines.

Acknowledgements

The authors thank H. Hara (Toyama Inc.) for designing a photoelectron shield and K. Horiba, M. Kitamura, K. Mase (KEK), and two anonymous reviewers for constructive comments. Performance evaluations were carried out at the Photon Factory (proposal No. 2019PF-17, 2019G609).

Funding information

This work was, in part, supported by a Grant-in-Aid for Scientific Research on Innovative Areas 'Aqua planetology' (JSPS KAKENHI grant No. JP17H06458).

References

Becker, K. B. (1992). *Rev. Sci. Instrum.* **63**, 1420–1423.
Belkhou, R., Stanescu, S., Swaraj, S., Besson, A., Ledoux, M., Hajlaoui, M. & Dalle, D. (2015). *J. Synchrotron Rad.* **22**, 968–979.
Bilderback, D. H., Freund, A. K., Knapp, G. S. & Mills, D. M. (2000). *J. Synchrotron Rad.* **7**, 53–60.
Boller, K., Haelbich, R.-P., Hogrefe, H., Jark, W. & Kunz, C. (1983). *Nucl. Instrum. Methods Phys. Res.* **208**, 273–279.
Freund, A. K., de Bergevin, F., Marot, G., Riekel, C., Susini, J., Zhang, L. & Ziegler, E. (1990). *Opt. Eng.* **29**, 928–941.
Henke, B. L., Gullikson, E. M. & Davis, J. C. (1993). *At. Data Nucl. Data Tables*, **54**, 181–342.
Krause, M. O. (1979). *J. Phys. Chem. Ref. Data*, **8**, 307–327.
Mairs, T., Baker, R., Clavel, C., Dabin, Y., Berard, L. E., Mattenet, M. & Guillemin, J. (2010). *Diamond Light Source Proc.* **1**, e38.
Ohashi, H., Senba, Y., Yumoto, H., Koyama, T., Miura, T. & Kishimoto, H. (2016). *AIP Conf. Proc.* **1741**, 040023.
Ohresser, P., Otero, E., Choueikani, F., Chen, K., Stanescu, S., Deschamps, F., Moreno, T., Polack, F., Lagarde, B., Daguerre, J.-P., Marteau, F., Scheurer, F., Joly, L., Kappler, J.-P., Muller, B., Bunau, O. & Sainctavit, Ph. (2014). *Rev. Sci. Instrum.* **85**, 013106.
Sasaki, S., Kakuno, K., Takada, T., Shimada, T., Yanagida, K. & Miyahara, Y. (1993). *Nucl. Instrum. Methods Phys. Res. A*, **331**, 763–767.
Schlachter, A. S. & Wuilleumier, F. J. (1994). *New Directions in Research with Third-Generation Soft X-ray Synchrotron Radiation Sources.* Maratea: Kluwer Academic Publishers.
Seah, M. P. & Dench, W. A. (1979). *Surf. Interface Anal.* **1**, 2–11.
Tanaka, T. & Kitamura, H. (2001). *J. Synchrotron Rad.* **8**, 1221–1228.
Toyoshima, A., Kikuchi, T., Tanaka, H., Adachi, J., Mase, K. & Amemiya, K. (2012). *J. Synchrotron Rad.* **19**, 722–727.
Watts, B., Pilet, N., Sarafimov, B., Witte, K. & Raabe, J. (2018). *J. Instrum.* **13**, C04001.